LA-UR-21-27898
Approved for public release; distribution is unlimited.

Title: Simulating PBX 9501 Gap-stick Experiment

Author(s): Menikoff, Ralph

Intended for: Report

Issued: 2021-08-10 (rev.1)

Simulating PBX 9501 Gap-stick Experiment

Ralph Menikoff

August 10, 2021

1 Introduction

The standard gap test, see for example [Gibbs and Popolato, 1980, part II, §4.2], utilizes a detonation wave in a donor HE attenuated by a gap (inert material) to shock load an acceptor HE. Due to the release wave following the donor detonation front, the gap is subject to a lead shock followed by a rarefaction wave. The thicker the gap, the more the rarefaction attenuates the lead shock and the lower the pressure that matches into the acceptor. A series of experiments is performed to determine the threshold thickness of the gap for which the acceptor HE detonates. For a specified donor HE and gap material, the threshold thickness of the gap is used as a measure of the relative sensitivity of acceptor HEs to shock ignition; *i.e.*, a more sensitive HE would have a larger threshold.

The gap-stick experiment, developed by Hill et al. [2016], utilizes an alternating sequence of cylindrical HE pellets and inert gaps. The pellets are all of the same HE with the same length. The gap lengths are increasing in the direction of wave propagation. The experiment involves the propagation of a detonation wave that is interrupted by each gap and reignites in the following HE pellet. It is like a sequence of gap experiments in which the lead shock pressure entering the subsequent HE pellets decreases. The lengths of the gaps are chosen such that reignition of the detonation wave fails before the last pellet.

The experiment measures the arrival times of the lead wave at the HE/gap interfaces. Polyvinylidene fluoride (PVDF or kynar®) polymer is a good shock impedance match for PBXs and used as the gap material. Instead of shorting pins along the outer surface of the cylinder, thin crystalline films of PVDF between the HE and the gap layers are used as piezoelectric gauges; see [Preston et al., 2015, slide 5]. The gauge responds to pressure anywhere across the cross sectional area of the gap-stick. Due to a rarefaction from the side boundary, the lead wave is bowed out and the gauge is effectively a timing pin on the axis.

Typically, in the shock initiation regime, reactive burn models are calibrated to data from shock-to-detonation transition (SDT) experiments. The data consists of the lead shock trajectory (from which a Pop plot data point is derived) and embedded velocity gauge profiles. These experiments are effectively 1-D and the detonation is initiated by a sustained shock. The gap-stick experiment provides data for more complicated shock loading; *i.e.*, pressure gradient

following a curved lead shock. It can be used to either test burn models for shock initiation over a wider range of loading conditions or used in the calibration of burn models.

It has previously been shown that the rate parameters of the SURF reactive burn model can be adjusted to fit the gap-stick data for PBX 9501 [Johnson et al., 2018, fig 4]. A recent re-calibration of the SURF model for PBX 9501 (lot 730-010 at $\rho = 1.837\,\mathrm{g/cc}^3$) used different reactants and products EOS and an updated fitting form for the burn rate [Menikoff, 2021]. The new calibration fit gap-stick data [Hill et al., 2021] together with data from SDT experiments and curvature effect data. Here the results of gap-stick simulations using the xRage code are shown. They provide insight into the reactive flow in the gap-stick experiment.

2 Gap-stick simulation

Gap-stick simulations have been run for experiment GST-6 [Hill et al., 2021]. In this experiment, the HE is PBX 9501 (lot 730-007 at $\rho = 1.833\,\mathrm{g/cc}^3$) and the inert gap material is PVDF. The gap-stick cylinder is a half inch diameter. The nominal length of the HE pellets is half inch long, and the gaps varied in length from 5.5 mm to 9 mm in increments of 0.5 mm. The simulations matched the initial setup shown in [Hill et al., 2021, fig 1] with the actual lengths of the pellets and gaps listed [Hill et al., 2021, fig 4].

The simulations used the xRage code with the SURF model for the HE and an adaptive mesh cell size down to 0.016 mm for the PBX 9501 reaction zone. The SURF rate parameters for PBX 9501 are from [Menikoff, 2021]. The Davis reactants and products EOS parameters are from [Aslam et al., 2020]. A Mie-Grüneisen Steinberg EOS model is used for the PDVF, with parameters given in Appendix A.

The principal measurement is the arrival times at the HE/inert interfaces from the PVDF gauges. The arrival times are obtained from numerical probe points on the axis. They are used to generate a Velocity Thickness Effect (V-TE) plot shown in fig. 1. The average HE wave

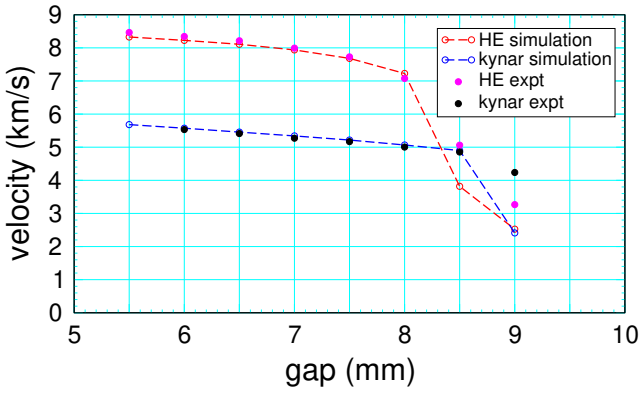

Figure 1: Average wave velocity across each HE pellet and each gap as a function of the gap thickness for each gap-HE cycle. Experimental data from [Hill et al., 2021, figs 4 and 6].

speed decreases as the time delay to detonate increases following longer gaps, and then drops precipitously after the 8 mm gap indicating that the detonation wave failed to reignite. The smaller drop for the experiment implies that some burning occurred in the pellet that failed while less burning occurred in the simulation.

A sequence of pressure profiles on axis at 0.5 μs time intervals for the last 2 re-ignition cycles is shown in fig. 2, and 2-D plots of density and pressure at selected times are shown in fig. 3. The 2-D plots show that the lead wave is curved, and that the transition to detonation in the HE pellet following the 8 mm gap occurs in a neighborhood of the axis and then spreads out radial; see plots at $t = 21$, 21.5 and 22.5 .

The 1-D pressure profiles shows the detonation wave in the PBX 9501 pellets. It has a thin reaction zone (spike in the profile) followed by a release wave with a steep pressure gradient. The detonation wave drives a shock wave in the following gap. Due to the steep gradient, the lead shock pressure drops well below the CJ pressure within the first few mm; see profiles at $t = 22.5$ and 23. Then the lead shock pressure decrease more slowly till it impacts the next HE pellet. At the end of the 8 mm and 8.5 mm gaps, the lead shock pressures falls to 10 and 8 GPa, respectively. Since PDVF is a good shock impedance match for PBX 9501, these are about the shock pressures entering the next pellet. The profile plot shows that with the pressure gradient behind the lead shock and the curved front, the threshold shock pressure for re-ignition is between 8 and 10 GPa.

Qualitatively the re-ignition for each gap is the same as fig. 2 and fig. 3 show for the 8 mm gap. A plot (not shown) shows that at the end of the 6 mm gap the lead shock pressure is about 15 GPa. Thus, the initial shock pressure in the HE pellets for the gap-stick experiment GST-6 span the range from 8 to 15 GPa. We note that the PBX 9501 Pop plot data [Gibbs and Popolato, 1980, pp 353-358] have initial shock pressures in the range from 2 to 8 GPa. The embedded gauge experiments used in the calibration of PBX 9501 have a smaller range of shock pressures; 3.1 to 5.2 GPa, see [Gustavsen et al., 1999, table 3]. Thus, the gap-stick experiments provide shock initiation data in a higher pressure range than the shock-to-detonation experiments used to calibrate rate models in the shock initiation regime. The trade-off is that the gap-stick

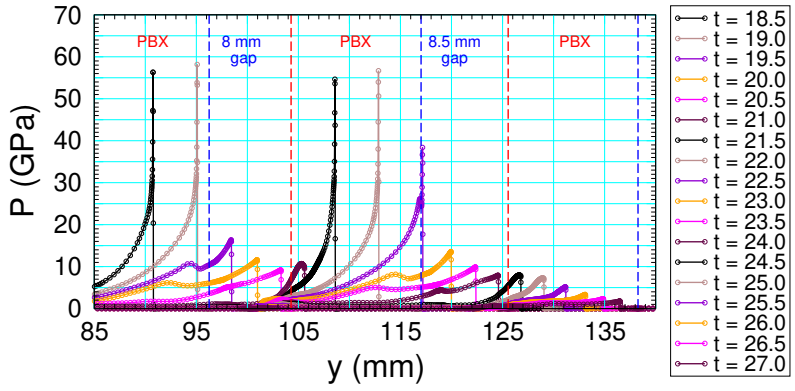

Figure 2: Sequence of simulated pressure profiles on axis for the last 2 re-ignition cycles before failure following the 8.5 mm gap. Legend gives time in microseconds.

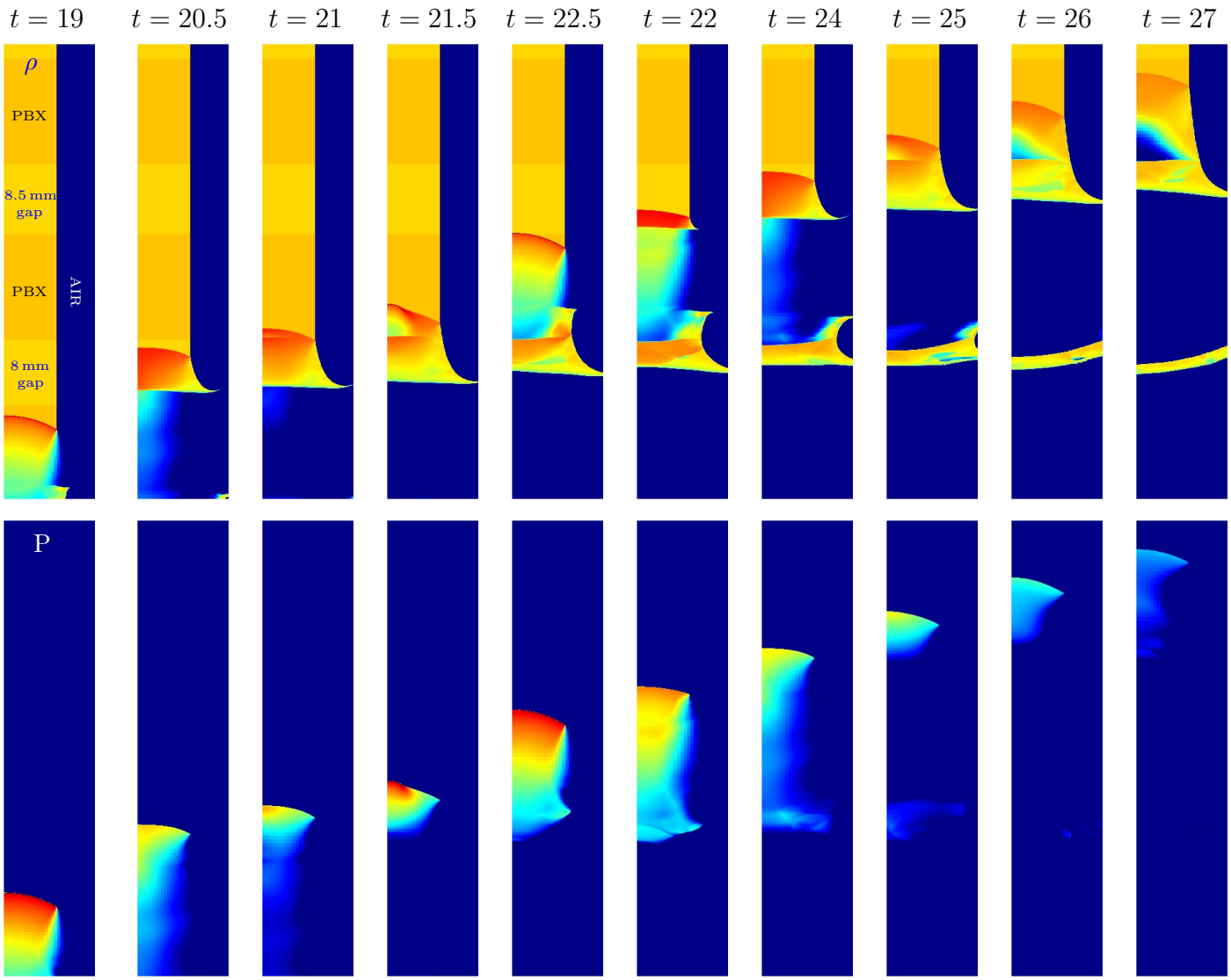

Figure 3: 2-D color plots at selected times of density and pressure, top and bottom, respectively. The portion of the simulation mesh plotted covers region about the 8 and 8.5 mm gaps; $0 < r < 12$ mm and $85 < y < 140$ mm with the cylindrical axis on the left. The plots use a rainbow color palette on a log scale; from low of blue to high of red. The density range is from 0.6 to 3 g/cc, and the pressure range from 0.4 to 40 GPa. The density scale is cutoff at 0.6 g/cc in order to have sufficient contrast to distinguish the initial densities of the PBX (orange) and gap material (yellow), 1.837 and 1.78 g/cc, respectively. Consequently, for the density plots, hot expanded detonation products are not distinguishable from the low density air (dark blue) surrounding the gap-stick.

experiment is more complicated; 2-D flow driven by a curved shock followed by a rarefaction rather than 1-D flow driven by a sustained shock.

Acknowledgement

The author thanks Larry Hill and Carl Johnson for discussion of the gap stick experiment and simulations for PBX 9501.

Appendices

A PVDF EOS

For PVDF (polyvinylidene fluoride) a Mie-Grüneisen EOS is used based on the Steinberg non-linear u_s-u_p form for the shock locus

$$u_s = c_0 + s(u_p/u_s) * u_p \ , \tag{1a}$$
$$s(u_p/u_s) = s_1 + s_2 * (u_p/u_s) + s_3 * (u_p/u_s)^2 \ , \tag{1b}$$
$$u_p/u_s = (V_0 - V)/V_0 \ , \tag{1c}$$
$$\Gamma/V = \Gamma_0/V_0 + b * (1/V - 1/V_0) \ . \tag{1d}$$

The EOS parameters in Table 1 have been fit shock data in [Marsh, 1980, p 477]. The principal shock locus in the (u_p,u_s)- and (V,P)-plane are plotted in fig. 4.

Table 1: Steinberg parameters for PVDF.

ρ_0	1.78	g/cc
c_0	1.850	km/s
s_1	3.72597	–
s_2	-7.10143	–
s_3	5.81222	–
Γ_0	0.8	–
b	0.0	–

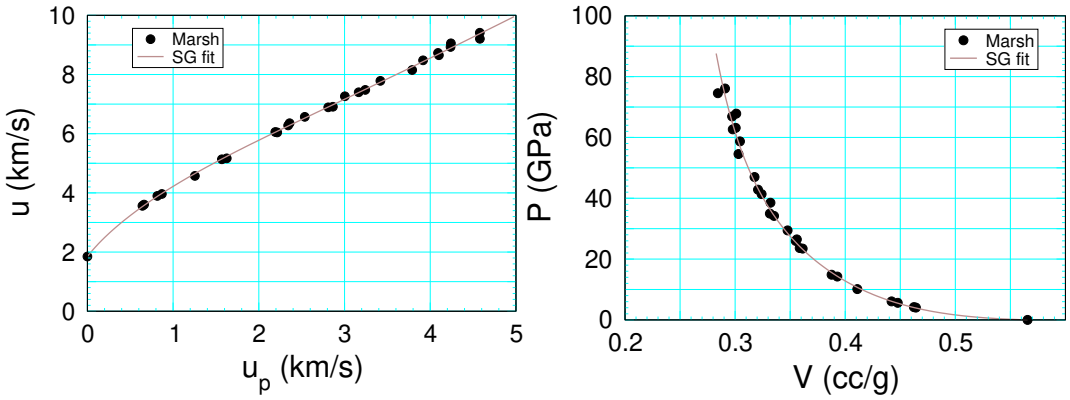

Figure 4: Shock locus for PVDF based on Steinberg EOS model. Data points from [Marsh, 1980, p 477]

References

T. D. Aslam, M. A. Price, C. Ticknor, J. D. Coe, J. A. Leiding, and M. A. Zonker. AWSD calibration for the HMX based explosive PBX 9501. In *AIP conference proceedings*, 2020. URL https://doi.org/10.1063/12.0000891.

T. R. Gibbs and A. Popolato, editors. *LASL Explosive Property Data*. Univ. of Calif. Press, 1980. URL http://lib-www.lanl.gov/ladcdmp/epro.pdf.

R. L. Gustavsen, S. A. Sheffield, R. R. Alcon, and L. G. Hill. Shock initiation of new and aged PBX 9501 measured with embedded electromagnetic particle velocity gauges. Technical Report LA-13634-MS, Los Alamos National Lab., 1999. URL https://doi.org/10.2172/10722.

L. Hill, R. Burritt, M. Herman, and J. Lichthardt. Gapstick results for PBX 9501 (GST-6). Technical Report LA-UR-21-24251, Los Alamos National Lab., 2021.

L. G. Hill, D. N. Preston, C. Johnson, and A. E. Hill. The Los Alamos Gapstick Test. In *Proc 47th Annual Conference of the Fraunhofer ICT*, pages pp 1–1 to 1–12, 2016.

C. E. Johnson, L. G. Hill, and D. N. Preston. Modeling the LANL gapstick experiment in PBX 9501 with the FLAG hydrocode. In *Proceeding of the Sixteenth International Symposium on Detonation*, pages pp 1118–1123, 2018.

S. P. Marsh, editor. *LASL Shock Hugoniot Data*. Univ. of Calif. Press, 1980.

R. Menikoff. Re-calibration of PBX 9501 SURF model. Technical Report LA-UR-21-27882, Los Alamos National Lab., 2021.

D. N. Preston, L. G. Hill, C. Johnson, and A. E. Hill. The Los Alamos Gap Stick Test. Technical Report LA-UR-15-24476, Los Alamos National Lab., 2015. Slides for talk at APS conference Shock Compression of Condensed Matter.